arXiv:hep-ph/0204250v3 15 Nov 2002

Static potential in baryon in the method of field correlators

D.S.Kuzmenko

State Research Center
Institute of Theoretical and Experimental Physics,
117218, B. Cheremushkinskaya 25, Moscow, Russia

Abstract

The static three-quark potential in arbitrary configuration of quarks is calculated analytically. It is shown to be in a full agreement with the precise numerical simulations in lattice QCD. The results of the work have important application in nuclear physics, as they allow to perform accurate analytic calculations of spectra of the baryons.

1 Introduction

Precise knowledge of the nucleon spectroscopy is very important for the deep understanding of the nuclear processes. The nonperturbative static potential is a key quantity in calculations of the baryon spectra, and this is why its investigation is one of the important problems in nuclear physics. Besides, the study of the static potential provides an insight into the two fundamental properties of strong interactions — confinement of the color charges and scale of the fluctuations of the confining gluonic fields.

In the present paper static potential in baryon is calculated using the method of the field correlators (MFC) [1], which is based directly on QCD and operates with the vacuum averages of the correlators of the gluonic field strengths.

It is suggested in MFC that the gluonic fields play a twofold role in QCD. First, gluons propagate dynamically in the vacuum, and this process at small distances can be described by the pertubation theory. In particular, the interaction of the quarks due to the one-gluon-exchange leads to the color-coulomb interaction potential. Second, gluons in the vacuum form the nonperturbative condensate, which constitutes the background, where the perturbative gluons propagate.

Two-point (or bilocal) correlators of gluonic fields are parameterized in MFC by the scalar formfactors [2]. This parameterization gives rise to the area law for the Wilson loop at sufficiently large separations between color sources, which ensures confinement. The slope σ of the linear static potential between quark and antiquark, corresponding to the Wilson loop, is the main parameter of MFC. Using this the only parameter one can obtain in MFC the spectra of the mesons within the 5% accuracy [3]. The value of σ is determined phenomenologically from the slope of the Regge trajectories of mesons, and corresponds to the confinement radius.

The scalar formfactors of the background fields fall off exponentially, which reflects the stochastic nature of the confining fluctuations of the gluonic background field. The correlation

length of the background fields T_g is sometimes considered as the second parameter of the MFC, although it can generally be expressed through the σ [12]. Its value is small in comparison with the radius of confinement and negligible for mesons. The situation for baryons is different because of the correlations of the background fields near the string junction, which lead according to MFC to the decreasing slope of the potential at small and intermediate quark separations. There is another T_g-induced effect, which is considered in the present work, namely the potential difference between the configurations with the same length of the string, but different locations of quarks.

The appearence of recent accurate numerical calculations of the static three-quark potential in lattice QCD in quenched approximation [5, 6] allow to test analytic results of MFC. We perform this important test in the paper and find a complete agreement between MFC and lattice results.

Before to calculate the static potential, in the next section of the paper we consider the Wilson loop of the baryon, which in the case of the static quarks is the baryon Green function. We express vacuum average of the Wilson loop through the vacuum averages of bilocal correlators of the gluon field strength tensor and parameterize them according to MFC. A brief discussion of the gluon condensate value obtained from the ITEP sum rules and its relation with the MFC is also given. In third section the procedure of calculation of the potential is described, and its behavior is analized in comparison with the lattice data. In the concluding section a summary of the results obtained in the paper is given, and their perspective applications are discussed.

2 The baryon Wilson loop and its average in MFC

It is known that the gauge-invariant state of the baryon with quarks at points $x,\ y,\ z$ reads as

$$\Psi_B(x,y,z,Y) = \epsilon_{\alpha\beta\gamma}\Phi^{\alpha}_{\alpha'}(x,Y,C_1)\Phi^{\beta}_{\beta'}(y,Y,C_2)\Phi^{\gamma}_{\gamma'}(z,Y,C_3)q^{\alpha'}(x)q^{\beta'}(y)q^{\gamma'}(z), \qquad (1)$$

where $\alpha,\ \beta, ...$ are the color indexes of the fundamental representation of $SU(3)$,

$$\Phi^{\alpha}_{\beta}(x,y,C) = (P\exp ig\int_C A_\mu dz_\mu)^{\alpha}_{\beta} \qquad (2)$$

is a parallel transporter along the contour C, which connects points $x,\ y$ (P in (2) means the ordering of color matrices along the trajectory of integration); q and A are quark and gluon field operators, and Y is the point of the string junction. The baryon Green function is defined as a vacuum average

$$G_B(\bar{X},X) = \left\langle \Psi^{+}_B(\bar{X})\Psi_B(X)\right\rangle, \qquad (3)$$

where $X \equiv x,y,z,Y$. If quarks are static, the Green function becomes the Wilson loop $\mathcal{W}_B$, which reads as

$$\mathcal{W}_B = \left\langle \frac{1}{6}\epsilon_{\alpha\beta\gamma}\epsilon^{\alpha'\beta'\gamma'}\Phi^{\alpha}_{\alpha'}(C_1)\Phi^{\beta}_{\beta'}(C_2)\Phi^{\gamma}_{\gamma'}(C_3)\right\rangle. \qquad (4)$$

The contours $C_1,\ C_2,\ C_3$ and direction of the integration are shown in Fig. 1. The trajectory of the string junction, which we denote C_0, is shown in the Fig. 1 by the dotted

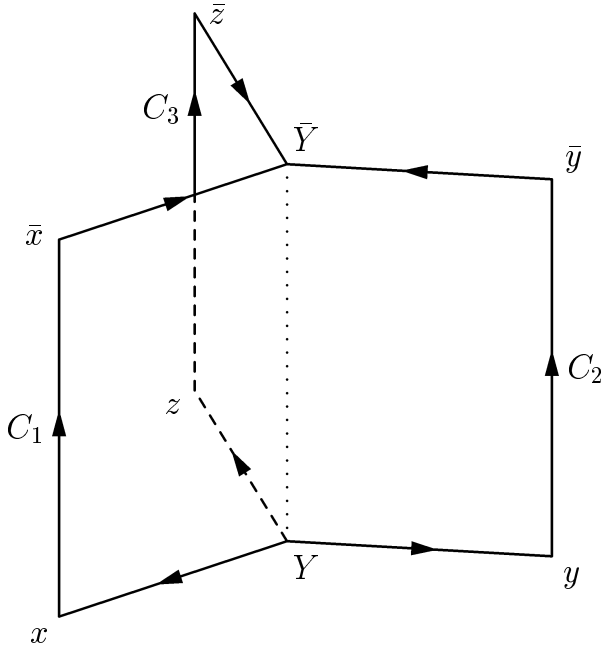

Figure 1: Baryon Wilson loop

line. Note that the definition (4) of the baryon Wilson loop is generally accepted. The static potential in baryon is related with the Wilson loop as follows,

$$V_B = -\lim_{T\to\infty} \frac{1}{T} \ln \mathcal{W}_B, \tag{5}$$

where T is the time extension of the Wilson loop.

We are now to express the Wilson loop (4) through the correlators of the gluon field strength tensor. For this sake rewrite it as

$$\mathcal{W}_B = \left\langle \frac{1}{6} \epsilon_{\alpha\beta\gamma} \epsilon^{\alpha'\beta'\gamma'} \Phi^{\alpha}_{\alpha'}(\tilde{C}_1) \Phi^{\beta}_{\beta'}(\tilde{C}_2) \Phi^{\gamma}_{\gamma'}(\tilde{C}_3) \right\rangle, \tag{6}$$

where $\tilde{C}_i = C_i \cup C_0$. The expression (6) follows from (4) after the substitution the latter with the equation

$$\epsilon^{\alpha'\beta'\gamma'} = \epsilon^{\alpha''\beta''\gamma''} \Phi^{\alpha''}_{\alpha'}(C_0) \Phi^{\beta''}_{\beta'}(C_0) \Phi^{\gamma''}_{\gamma'}(C_0). \tag{7}$$

Note that the last relation is valid in the generalized coordinate gauge, in which $\Phi^{\alpha}_{\alpha'}(C_0) = \delta^{\alpha}_{\alpha'}$, but the expression (6) is a scalar of the color $SU(3)$ and therefore does not depend on the choice of the gauge. Since the integration in (6) is performed along three closed contours, one may use for these contours of the baryon Wilson loop the nonabelian Stokes theorem [1]. As a result one gets

$$\mathcal{W}_B = \left\langle \frac{1}{6} \epsilon_{\alpha\beta\gamma} \epsilon^{\alpha'\beta'\gamma'} W^{\alpha}_{\alpha'}(S_1) W^{\beta}_{\beta'}(S_2) W^{\gamma}_{\gamma'}(S_3) \right\rangle, \tag{8}$$

where S_i are the minimal surfaces of the contours $\tilde{C}_i$, and

$$W^{\alpha}_{\alpha'}(S) = \mathcal{P} \exp(ig \int_S d\sigma_{\mu\nu}(x) F_{\mu\nu}(x) \Phi(x, x_0))^{\alpha}_{\alpha'} \tag{9}$$

does not depend on the choice of the point x_0, if the latter places at the surface S [1]. Expand now the exponent in (9),

$$W^{\alpha}_{\alpha'}(S) = \delta^{\alpha}_{\alpha'} + ig\int_S d\sigma\, F^{\alpha}_{\alpha'} - \frac{g^2}{2}\int_S\int_S d\sigma(1)\, d\sigma(2)\, F^{\alpha}_{\beta}(1)F^{\beta}_{\alpha'}(2) + ..., \tag{10}$$

where we have explicitely written only the color indexes and denoted by the dots the higher powers of the expansion. Since the vacuum average of the strength tensor equals to zero, the Wilson loop will read as follows,

$$\mathcal{W}_B = \frac{1}{6}\epsilon_{\alpha\beta\gamma}\epsilon^{\alpha'\beta'\gamma'}\left(\delta^{\alpha}_{\alpha'}\delta^{\beta}_{\beta'}\delta^{\gamma}_{\gamma'} - \delta^{\beta}_{\beta'}\delta^{\gamma}_{\gamma'}\,\frac{g^2}{2}\int_{S_1}\int_{S_1} d\sigma(1)\, d\sigma(2)\, F^{\alpha}_{\rho}(1)F^{\rho}_{\alpha'}(2) - \right.$$

$$\left. - \,\delta^{\gamma}_{\gamma'}\, g^2\int_{S_1}\int_{S_2} d\sigma(1)\, d\sigma(2)\, F^{\alpha}_{\alpha'}(1)F^{\beta}_{\beta'}(2) + ...\right), \tag{11}$$

where the dots denote the double integrals over surfaces S_2S_2, S_3S_3, S_1S_3, and S_2S_3, analogous to the written ones, as well as the higher order correlators. Taking into account that $\epsilon_{\alpha\beta\gamma}\epsilon^{\alpha'\beta\gamma}F^{\alpha}_{\rho}F^{\rho}_{\alpha'} = 2\,\mathrm{tr}\,FF$, $\epsilon_{\alpha\beta\gamma}\epsilon^{\alpha'\beta'\gamma}F^{\alpha}_{\alpha'}F^{\beta}_{\beta'} = -\mathrm{tr}\,FF$, one gets from (11)

$$\mathcal{W}_B = \exp\left\{-\sum_{i=1}^{3}\frac{1}{2}\int_{S_i}\int_{S_i} d\sigma(1)d\sigma(2)\left\langle\frac{g^2}{3}\mathrm{tr}F(1)F(2)\right\rangle + \right.$$

$$\left. + \sum_{i<j}\frac{1}{2}\int_{S_i}\int_{S_j} d\sigma(1)d\sigma(2)\left\langle\frac{g^2}{3}\mathrm{tr}F(1)F(2)\right\rangle\right\}. \tag{12}$$

Here and in what follows we disregard the higher order correlators, assuming that their contribution to Wilson loop is small or can be reduced to the contribution of the bilocal ones. This assumption leads to the area law for the Wilson loop and is shown in [7] to be motivated by the property of the Casimir scaling of the potentials of static sources in various representations of $SU(3)$.

The second motivation of the cancellation of the contributions of higher order correlators to the Wilson loop follows from the stochastic properties of the QCD vacuum. Note that the bilocal correlators written in (12) are the first term of the cluster expansion used in the theory of fluctuations [9] for the description of the correlated stochastic processes. According to the fundamental identity of the cluster expansion, higher order correlators enter into (12) as cumulants, or connected correlators (one can find an accurate definition of cumulants as well as the proof of the fundamental identity in [9]), which rapidly fall off with the increasing order for almost independent points. That's why the bilocal approximation taking into account only two-point correlators is motivated by the theory of fluctuations at distances greater than the correlation length of the gluon fields.

The bilocal correlators are parameterized in MFC [2] in the case of $SU(N_c)$ using two scalar formfactors D and D_1 as follows,

$$\frac{g^2}{N_c}\mathrm{tr}\langle F_{\mu_1\nu_1}(x)\Phi(x,x')F_{\mu_2\nu_2}(x')\Phi(x',x)\rangle = (\delta_{\mu_1\mu_2}\delta_{\nu_1\nu_2} - \delta_{\mu_1\nu_2}\delta_{\mu_2\nu_1})D(z) +$$

$$+\frac{1}{2}\left(\frac{\partial}{\partial z_{\mu_1}}(z_{\mu_2}\delta_{\nu_1\nu_2} - z_{\nu_2}\delta_{\nu_1\mu_2}) + \frac{\partial}{\partial z_{\nu_1}}(z_{\nu_2}\delta_{\mu_1\mu_2} - z_{\mu_2}\delta_{\mu_1\nu_2})\right)D_1(z) \equiv \mathcal{D}_{\mu_1\nu_1,\mu_2\nu_2}(z), \tag{13}$$

where $z \equiv x - x'$. The formfactors of the background fields read as

$$D(z) = D(0) \exp\left(-\frac{|z|}{T_g}\right), \quad D_1(z) = D_1(0) \exp\left(-\frac{|z|}{T_g}\right). \tag{14}$$

The exponential behavior of the formfactors is confirmed by the lattice simulations [10, 11] at distances $z \gtrsim 0.2$ fm. The values of the parameters obtained are $T_g = 0.12 \div 0.2$ fm [10, 11] and $D_1(0)/D(0) \approx 1/3$ [10].

In the case of static quark and antiquark the relation analogous to (12) reads as

$$\mathcal{W}_B = \exp\left\{-\frac{1}{2}\int_S\int_S d\sigma(1) d\sigma(2) \left\langle \frac{g^2}{N_c} \mathrm{tr} F(1) F(2) \right\rangle\right\} \tag{15}$$

and at large quark separations $R \gg T_g$ gives rise to the area law for the Wilson loop,

$$\langle \mathcal{W} \rangle^{\mathrm{biloc}} = \exp(-\sigma S), \tag{16}$$

where the string tension σ is given by the relation

$$\sigma = \frac{\pi}{2}\int_0^\infty dz^2\, D(z). \tag{17}$$

The value of the string tension $\sigma \approx 0.18\ \mathrm{GeV}^2$ may be determined phenomenologically from the slope of the meson Regge trajectories [3]. Note that the value $T_g \approx 0.13$ fm can be extracted from the gluelump spectrum, which is calculated in MFC [12] using the only nonperturbative parameter σ.

From (13) and (14) the equation

$$\left\langle \frac{\alpha_s}{\pi} F^a_{\mu\nu}(x) F^a_{\mu\nu}(0) \right\rangle = \frac{18 D(x)}{\pi^2} \tag{18}$$

follows, which relates in particular the gluon condensate $\left\langle \frac{\alpha_s}{\pi} F^a_{\mu\nu}(0) F^a_{\mu\nu}(0) \right\rangle \equiv \left\langle \frac{\alpha_s}{\pi} F^2 \right\rangle$ with the value of the formfactor D at zero. Although $D(0)$ does not enter formally into the definition of σ (17), but assuming the behaviour of $D(z)$ (14) at small distances (this assumption is rigorously speaking false [13], nevertheless we use it in this paper as an approximation; the accurate expressions at small distances can be found in [14]), one gets $\sigma = \pi D(0) T_g^2$, which allows to evaluate the gluon condensate as follows, $\left\langle \frac{\alpha_s}{\pi} F^2 \right\rangle = 18\,\sigma/(\pi^3 T_g^2) \approx 0.25\ \mathrm{GeV}^4$, for $T_g = 0.13$ fm.

The value of the gluon condensate can also be obtained from the ITEP sum rules (see the book [15] and references to the original works therein). The sum rules use the operator expansion for the currents, and the gluon condensate contribute to it in combination $\left\langle \frac{\alpha_s}{\pi} G^2 \right\rangle / Q^4$. Herewith the value of the gluon condensate is assumed to be independent on the momentum. Recently on the basis of the analysis using the sum rules of the experimental data on τ-lepton decays and charmonium spectrum in the papers [16] were obtained the following values of gluon condensate: $\left\langle \frac{\alpha_s}{\pi} G^2 \right\rangle = (0.006 \pm 0.012)\ \mathrm{GeV}^4$ and $\left\langle \frac{\alpha_s}{\pi} G^2 \right\rangle = (0.009 \pm 0.007)\ \mathrm{GeV}^4$ correspondingly.

One can assume that the sum rules operate with the some effective value of the condensate, which equals to the correlator $\left\langle \frac{\alpha_s}{\pi} F^a_{\mu\nu}(x_{\mathrm{ef}}) F^a_{\mu\nu}(0) \right\rangle$ at some effective separation $x_{\mathrm{ef}} \neq 0$. Taking $\left\langle \frac{\alpha_s}{\pi} G^2 \right\rangle = 0.007\ \mathrm{GeV}^4$ and $T_g \approx 0.13$ fm, one obtains $x_{\mathrm{ef}} = T_g \ln\left(\left\langle \frac{\alpha_s}{\pi} F^2 \right\rangle / \left\langle \frac{\alpha_s}{\pi} G^2 \right\rangle\right) \approx 0.5$ fm, i.e. characteristic radius of confinement. Note that when assuming that bilocal

correlators do not depend on point separation and $D(x)$=const, and integrating in (17) up to the characteristic hadronic size $r_h = 1$ fm, one can estimate the gluon condensate from (17), (18) as $\left\langle \frac{\alpha_s}{\pi} F^2 \right\rangle \approx \sigma / r_c^2 \approx 0.007$ GeV^4, which is also consistent with the value obtained in [16].

The conclusion is that the sum rules results can not be used neither as a confirmation nor as a disclaimer of the MFC parameterization (14).

3 The baryon potential

According to (5), (12), (14) the baryon potential reads as

$$V_B = \lim_{T\to\infty} \frac{1}{2} \sum_{a=1,2,3} \int_{S_a}\int_{S_a} d\sigma^{(a)}_{\mu_1\nu_1}(x) d\sigma^{(a)}_{\mu_2\nu_2}(x') \mathcal{D}_{\mu_1\nu_1,\mu_2\nu_2}(x-x') -$$

$$- \frac{1}{2} \sum_{a<b} \int_{S_a}\int_{S_b} d\sigma^{(a)}_{\mu_1\nu_1}(x) d\sigma^{(b)}_{\mu_2\nu_2}(x') \mathcal{D}_{\mu_1\nu_1,\mu_2\nu_2}(x-x'), \qquad (19)$$

where $d\sigma^{(a)}$ denotes an integration over the surface S_a. Note that the nondiagonal part of the potential (i.e. second term in (19) at $a \neq b$) differs in the factor $-1/2 = -1/(N_c - 1)$ from the corresponding quantity in [17, 18], where the error was made by the author (in eqs.(24) from [17] and (46) from [18]).

Since the surfaces of the Wilson loop are oriented along the temporal axis, only correlators of the color-electric field contribute to the potential (19), and one gets

$$V_B(R_1, R_2, R_3) = \left(\sum_{a=b} - \sum_{a<b} \right) n_i^{(a)} n_j^{(b)} \int_0^{R_a}\int_0^{R_b} dl\, dl' \int_0^\infty dt\, \mathcal{D}_{i4,j4}(z_{ab}), \qquad (20)$$

where $\mathbf{n}^{(a)}$ is a vector of unit length directed along the line connecting string junction with the corresponding quark; $z_{ab} = (l\,\mathbf{n}^{(a)} - l'\mathbf{n}^{(b)}, t)$, R_a is a distance from the string junction to the corresponding quark, and

$$\mathcal{D}_{i4,j4}(z) = \delta_{ij} D(z) + \frac{\partial}{\partial z_i} \frac{z_j D_1(z)}{2}. \qquad (21)$$

In what follows we neglect the formfactor D_1 in (21), since its contribution to the potential is small.

In calculation of the baryon potential one should distinguish configurations of quarks, in which quarks form 1) triangles with each of the angles less that $2\pi/3$ and 2) triangles having one angle greater than $2\pi/3$. In the former case the minimal surface of the Wilson loop consists of three surfaces intersecting with each other at angles $2\pi/3$, as is shown in Fig. 1. In the latter one the string junction position coincide with the position of quark at large angle, and the Wilson loop consists of two surfaces. Then one can set in Eq. (20) $R_3 = 0$.

Consider in advance configuration of the equilateral triangle. In this case $R_1 = R_2 = R_3 \equiv R$, and baryon potential reads as

$$V_B(R) = 3V_M(R) + V_{\rm nd}(R), \qquad (22)$$

where V_M is diagonal and $V_{\rm nd}$ nondiagonal terms. From eqs.(14), (20),(21) one gets

$$V_M(R) = 2D(0) \int_0^R d\,z_1 (R - z_1) \int_0^\infty d\,t \exp\left(-\frac{|z|}{T_g} \right) =$$

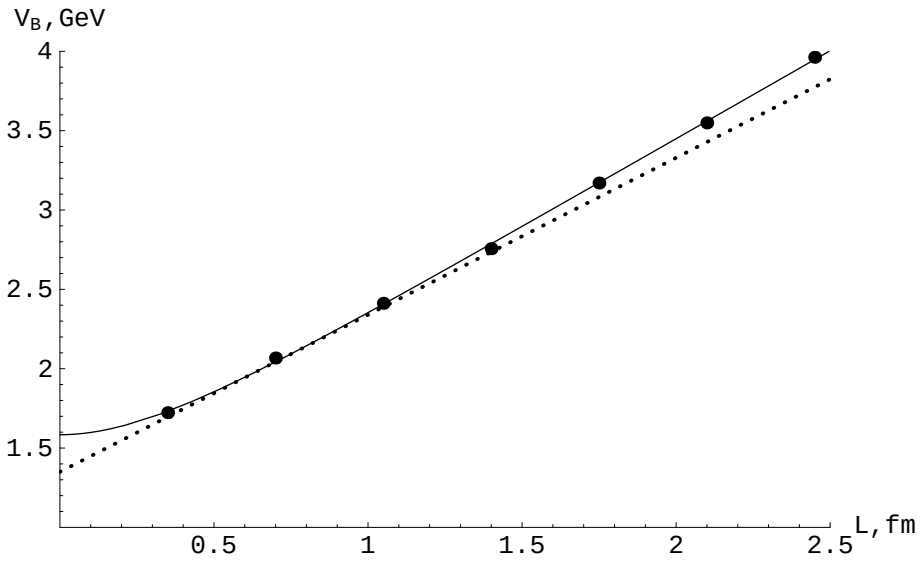

Figure 2: The lattice nonperturbative baryon potential from [5] (points) for lattice parameter $\beta = 5.8$ and MFC potential $V^{(B)}$ (solid line) with parameters $\sigma = 0.22$ GeV^2 and $T_g = 0.12$ fm vs. the minimal length of the string L. The dotted line is a tangent at $L = 0.7$ fm.

$$= \frac{2\sigma}{\pi}\left\{R\int_0^{R/T_g} d\,x\,xK_1(x) - T_g\left(2 - \frac{R^2}{T_g^2}K_2\left(\frac{R}{T_g}\right)\right)\right\}, \tag{23}$$

where $\sigma = \pi D(0)T_g^2$, K_1 and K_2 are McDonald functions. This potential determines an interaction of static quark and antiquark at separation R. Note that it is related with the gluon field in meson calculated in MFC [18] using the connected probe as follows,

$$\frac{dV_M(R)}{dR} = \frac{2\sigma}{\pi}\int_0^{R/T_g} dx\,x\,K_1(x) \equiv E_0(R), \tag{24}$$

where $E_0(R)$ is a value of the confining field acting on the quark.

The nondiagonal potential,

$$V_{\rm nd}(R) = \frac{2}{\sqrt{3}}\sigma T_g - \frac{3\sqrt{3}}{2\pi}\frac{\sigma R^2}{T_g}\int_{\frac{\pi}{6}}^{\frac{\pi}{3}}\frac{d\,\varphi}{\cos\varphi}K_2\left(\frac{\sqrt{3}R}{2T_g\cos\varphi}\right), \tag{25}$$

is positive, rises from zero to the value $2/\sqrt{3}\,\sigma T_g$, and saturates at $R \gtrsim 0.6$ fm.

The behavior of the potential (22) versus the minimal length of the baryon string $L = R_1 + R_2 + R_3 = 3R$ is shown in Fig. 2 in comparison with the lattice data from [5]. One can see that the potential completely describes the lattice results. At large distances $L \gtrsim 1.5$ fm the potential rises linearly with the slope σ. At characteristic hadronic sizes the slope of the potential falls, which is shown in Fig. 2 by the tangent at point $L = 0.7$ fm with the slope $\sim 0.9\sigma$. Note that all lattice points at $L < 1.5$ fm are cosistent with the tangent. This effect is also confirmed by the phenomenology of baryon spectrum [19].

To perform the analysis of the lattice results from [6], one should add to the potential (22) the perturbative color-coulomb one,

$$V_{\rm pert} = -\frac{3}{2}\frac{C_F\alpha_s}{r}, \tag{26}$$

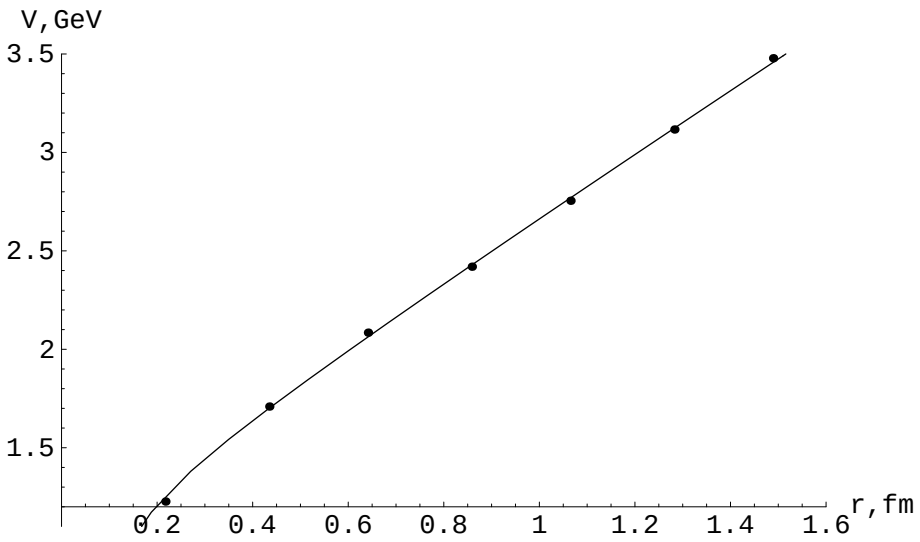

Figure 3: The lattice baryon potential in the equilateral triangle with quark separations r from [6] (points) at $\beta = 5.8$ and the MFC potential $V^{(B)} + V^{\rm pert}_{\rm (fund)}$ (solid line) at $\alpha_s = 0.18$, $\sigma = 0.18$ GeV^2, and $T_g = 0.12$ fm.

where $C_F = 4/3$ is the fundamental Casimir operator. The results are shown in Fig. 3. One can see the full agreement of our potential with this independent set of lattice data as well.

In the case of the triangle with different separations R_a of quarks from the string junction, having angles no larger than $2\pi/3$

$$V_B(R_1, R_2, R_3) = \sum_{a=1}^{3} V_M(R_a) + \sum_{a<b} V_{\rm nd}(R_a, R_b), \tag{27}$$

where

$$V_{\rm nd}(R_a, R_b) = \frac{2\sigma T_g}{3\sqrt{3}} - \frac{\sqrt{3}\sigma}{4\pi T_g} \left\{ R_a^2 \int_0^{\tilde\varphi_{ab}} \frac{d\,\varphi}{\cos^2\left(\varphi + \frac{\pi}{6}\right)} K_2\left(\frac{\sqrt{3}R_a}{2T_g \cos\left(\varphi + \frac{\pi}{6}\right)}\right) + \right.$$
$$\left. + R_b^2 \int_{\tilde\varphi_{ab}}^{\frac{\pi}{3}} \frac{d\,\varphi}{\sin^2\varphi} K_2\left(\frac{\sqrt{3}R_b}{2T_g \sin\varphi}\right) \right\}. \tag{28}$$

If one of the angles of the triangle is larger than $2\pi/3$, the position of string junction coincides with the position of quark at large vertex. Let us denote α an angle supplementary to the large one; $r_1,\ r_2$ the distances from the string junction to the adjacent quarks. Then we get

$$V_B(r_1, r_2, \alpha) = V_M(r_1) + V_M(r_2) + V_{\rm nd}(r_1, r_2, \alpha), \tag{29}$$

where

$$V_{\rm nd}(r_1, r_2, \alpha) = \frac{2\alpha\,{\rm ctg}\,\alpha}{\pi}\,\sigma T_g - \frac{\sin 2\alpha\,\sigma}{2\pi T_g} \left\{ r_1^2 \int_0^{\tilde\varphi} \frac{d\,\varphi}{\sin^2(\alpha - \varphi)} K_2\left(\frac{r_1 \sin\alpha}{T_g \sin(\alpha - \varphi)}\right) + \right.$$
$$\left. + r_2^2 \int_{\tilde\varphi}^{\alpha} \frac{d\,\varphi}{\sin^2\varphi} K_2\left(\frac{r_2 \sin\alpha}{T_g \sin\varphi}\right) \right\}. \tag{30}$$

Note that $V_{\rm nd}(r_1, r_2, \alpha) = V_{\rm nd}(r_2, r_1, \alpha)$; $\quad V_{\rm nd}(r_1, r_2, \pi/3) = V_{\rm nd}(r_1, r_2)$, $\quad V_{\rm nd}(R, R) = 1/3!\, V_{\rm nd}(R)$.

For the analysis of the dependence of potential on the location of quarks, let us consider its behavior in isoceles triangles with the vertex $0 \le \gamma \le \le 2\pi/3$ and fixed length of the string $L = R_1 + R_2 + R_3$ versus the value of γ. At distances $R_a \gtrsim 0.5$ fm one can use asymptotic formulas following from (23), (28) and (30),

$$V_M(R) \approx \sigma R - \frac{4}{\pi}\,\sigma T_g,$$

$$V_{\rm nd}(R_a, R_b) \approx \frac{2\sigma T_g}{3\sqrt{3}}, \qquad V_{\rm nd}(r_1, r_2, \alpha) \approx \frac{2\alpha\,{\rm ctg}\,\alpha}{\pi}\,\sigma T_g. \tag{31}$$

One can conclude that at $\gamma = 0$, when positions of two quarks coincide and these quarks are in the antitriplet of color $SU(3)$, the baryon potential in isoceles triangle reduces to the meson one,

$$V^L(\gamma = 0) \approx \sigma L - \frac{4}{\pi}\,\sigma T_g. \tag{32}$$

If $0 < \gamma < 2\pi/3$, then the string consists of three lengths and

$$V^L(0 < \gamma < 2\pi/3) \approx \sigma L + \left(-\frac{12}{\pi} + \frac{2}{\sqrt{3}}\right)\sigma T_g. \tag{33}$$

If the string consists of two lengths, then

$$V^L(\gamma \ge 2\pi/3) \approx \sigma L + \left(-\frac{8}{\pi} + \frac{2}{\pi}(\pi - \gamma)\,{\rm ctg}\,(\pi - \gamma)\right)\sigma T_g. \tag{34}$$

According to eqs. (32) – (34), when γ icreasing, the potential rapidly falls by the value

$$\Delta V_1 = \left(\frac{8}{\pi} - \frac{2}{\sqrt{3}}\right)\sigma T_g \approx 150\ {\rm MeV}, \tag{35}$$

almost does not change in the range $0 \lesssim \gamma \lesssim 2\pi/3$, then rapidly increases at $\gamma \approx 2\pi/3$ by the value

$$\Delta V_2 = \left(\frac{4}{\pi} - \frac{4}{3\sqrt{3}}\right)\sigma T_g \approx 55\ {\rm MeV}, \tag{36}$$

and slowly increases in the range $2\pi/3 \le \gamma \le \pi$ by the value

$$\Delta V_3 \equiv V^L(\pi) - V^L\left(\frac{2\pi}{3}\right) = \left(\frac{2}{\pi} - \frac{2}{3\sqrt{3}}\right)\sigma T_g \approx 30\ {\rm MeV}, \tag{37}$$

where numerical values are given for $\sigma = 0.18$ GeV^2, $T_g = 0.12$ fm. The dependence of the baryon potential in isoceles triangle on the angle γ at $L = 1.8$ fm is shown in Fig. 4. Note that character jumps and drops of the potential are proportional to the quantity σT_g, i.e. determined by confinement as well as by correlations of the stochastic nonperturbative fields, and it would be interesting to obtain them independently in lattice QCD. Baryon potential in various configurations of quarks was considered on the lattice in [5]. However, configurations with the angles in the range $\pi/20 \lesssim \alpha < \pi/2$ considered in this work did not allow to establish this dependence, because in the range of the small angles the size of lattice spacing becomes comparable with the quark separation and accurate calculations of the potential become difficult. The further lattice investigations of configurations with large angle are called for.

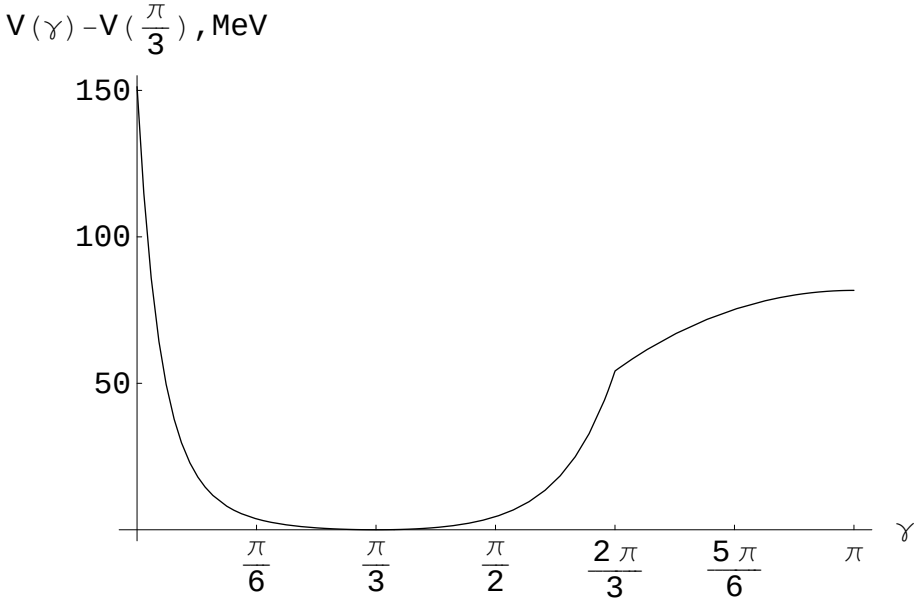

Figure 4: The baryon potential in isoceles triangle with the length of the string $L = 1.8$ fm versus the vertex γ for $\sigma = 0.18$ GeV^2, $T_g = 0.12$ fm.

It is also interesting to consider the energy density of the string near the string junction, or the quantity

$$\tilde{V}^L(\gamma) = \frac{1}{2}\left(\sum_{a=1}^{3} V_M(R_a) - \sigma L\right) + \sum_{a<b} V_{\rm nd}(R_a, R_b). \tag{38}$$

If the vertex in the isoceles triangle with the string length fixed is in the region $2\pi/3 \lesssim \gamma \lesssim \pi$, the potential $\tilde{V}^L(\gamma)$ has the same behavior as the $V^L(\gamma)$, since in this region the dependence of the latter on the value of vertex is determined by the only nondiagonal term. This means that while the vertex is increasing in this range, the energy density is rising. The drop at $\gamma = 0$ for $\tilde{V}$ is small,

$$\Delta\tilde{V}_1 = \left(\frac{4}{\pi} - \frac{2}{\sqrt{3}}\right)\sigma T_g = 0.12\sigma T_g \approx 13 \text{ MeV}. \tag{39}$$

At $\gamma = 2\pi/3$ the potential $\tilde{V}^L(\gamma)$ drops but not jumps as $V^L(\gamma)$ does,

$$\Delta\tilde{V}_2 = \left(\frac{2}{\pi} - \frac{4}{3\sqrt{3}}\right)\sigma T_g = -0.13\sigma T_g \approx -15 \text{ MeV}, \tag{40}$$

i.e. the energy density decreases. One can conclude that the energy density near the string junction depends on the location of the quarks only slightly. This is in contradiction with the field distributions obtained in [17, 18] using the connected probe, where author has made an error in the basic formulas (11)-(18) from [17] and (27) from [18]. It is not hard to show that the cited formulas and corresponding field distributions concern to the two or three static meson Wilson loops in the special case when the positions of antiquarks coincide, but not to baryons. The problem of the field distributions in baryon with the connected probe has some ambiguities and will be considered in subsequent publications.

4 Conclusions

In the present work the nonperturbative static potential in baryon was calculated analytically in the framework of MFC for arbitrary locations of quarks. Two important effects related with the correlations of the nonperturbative gluon fields are studied: a decrease of the slope of the potential at hadronic lengths, and its dependence on the locations of quarks when length of the string fixed. The latter effect is found for the first time and shown to be proportional to the combinations of parameters σT_g. It would be interesting to verify it independently on the lattice and extract an accurate value of the correlation length of gluonic fields.

The errors in preceding works [17, 18] were corrected for baryon potential and stated for the field distributions in baryon with the connected probe.

The dependence of the potential on the length of the string was shown in the paper to be in complete agreement with the precise numerical lattice calculations, which allows to perform the accurate analytic studies of the baryon spectra, first of all of the spectrum of nucleons, and has important meaning for various applications in nuclear physics.

The author is grateful to Yu.A.Simonov for numerous useful discussions. I also thank T.Takahashi, Ph.de Forcrand and V.I.Shevchenko for the correspondence. Partial support by RFBR grants 00-02-17836, 00-15-96786, and INTAS 00-00110, 00-00366 is acknowledged.

References

[1] A. Di Giacomo, H.G. Dosch, V.I. Shevchenko and Yu.A. Simonov, hep-ph/0007223.

[2] H.G. Dosch, Phys.Lett. **B190**, 177 (1987);
H.G. Dosch and Yu.A. Simonov, Phys.Lett. **B205**, 399 (1988);
Yu.A. Simonov, Nucl.Phys. **B307**, 512 (1988).

[3] A.Yu. Dubin, A.B. Kaidalov, and Yu.A. Simonov, Phys.Lett. **B323**, 41 (1994); Phys.Lett. **B343**, 310 (1995);
Yu.S. Kalashnikova, A.V. Nefediev, and Yu.A. Simonov, Phys.Rev. **D64**, 014037 (2001).

[4] Yu.A. Simonov, Nucl.Phys. **B592**, 350 (2000).

[5] T.T. Takahashi *et al.*, Phys.Rev. **D65**, 114509 (2002).

[6] C. Alexandrou, Ph. de Forcrand, and O. Jahn, hep-lat/0209062, talk presented at Lattice'2002.

[7] Yu.A.Simonov, **71**, 187 (2000), hep-ph/0001244;
V.I.Shevchenko and Yu.A.Simonov, Phys.Rev.Lett. **85**, 1811 (2000).

[8] G.S.Bali, Nucl.Phys. B (Proc.Suppl.) **83**, 422 (2000).

[9] N.G. Van Kampen, Stochastic Processes in Physics and Chemistry, North-Holland Physics Publishing, 1984.

[10] M. Campostrini, A. Di Giacomo and G. Mussardo, Z.Phys. **C25**, 173 (1984);
A. Di Giacomo and H. Panagopoulos, Phys.Lett. **B285** , 133 (1992);
A. Di Giacomo, E. Meggiolaro and H. Panagopoulos, Nucl.Phys. **B483** , 371 (1997).

[11] G.S. Bali, N. Brambilla, and A. Vairo, Phys.Lett. **B421**, 265 (1998).

[12] Yu.A. Simonov, Nucl.Phys. **B592**, 350 (2001).

[13] Yu.A. Simonov, Sov.J.Nucl.Phys. **50**, 134 (1989).

[14] Yu.A. Simonov, hep-ph/0205334.

[15] F.J. Yndurain, The Theory of Quark and Gluon Interactions, Springer-Verlag, 1999, p. 208.

[16] B.V. Geshkenbein, B.L. Ioffe, K.N. Zyablyuk, Phys.Rev. **D64,** 093009 (2001);
B.L. Ioffe, K.N. Zyablyuk, hep-ph/0207183;
B.L. Ioffe, hep-ph/0209313.

[17] D.S. Kuzmenko and Yu.A. Simonov, Phys.Lett. **B494**, 81 (2000).

[18] D.S. Kuzmenko and Yu.A. Simonov, Yad.Fiz. **64**, 110 (2001), hep-ph/0010114.

[19] S. Capstick, N. Isgur, Phys.Rev. D **34,** 2809 (1986).